



Citation for published version:

Pallipurath, A, Skelton, J, Bucklow, S & Elliott, S 2015, 'A chemometric study of ageing in lead-based paints', *Talanta*, vol. 144, pp. 977-985. <https://doi.org/10.1016/j.talanta.2015.07.037>

DOI:

[10.1016/j.talanta.2015.07.037](https://doi.org/10.1016/j.talanta.2015.07.037)

Publication date:

2015

Document Version

Peer reviewed version

[Link to publication](#)

Publisher Rights

CC BY-NC-ND

The published version is available via: <http://dx.doi.org/10.1016/j.talanta.2015.07.037>

University of Bath

General rights

Copyright and moral rights for the publications made accessible in the public portal are retained by the authors and/or other copyright owners and it is a condition of accessing publications that users recognise and abide by the legal requirements associated with these rights.

Take down policy

If you believe that this document breaches copyright please contact us providing details, and we will remove access to the work immediately and investigate your claim.

A chemometric study of ageing in lead-based paints

Anuradha Pallipurath,^{1,2} Jonathan Skelton,^{1,3} Spike Bucklow⁴ and Stephen Elliott^{1*}

¹*Department of Chemistry, University of Cambridge, Lensfield Road, CB2 1EW, Cambridge, UK.*

²*Present address: School of Chemistry, National University of Ireland, Galway, Ireland*

³*Present address: Department of Chemistry, University of Bath, Claverton Down, Bath, BA2 7AY, UK*

⁴*Hamilton-Kerr Institute, University of Cambridge, Mill Lane, Whittlesford, CB22 4NE, Cambridge, UK*

**To whom correspondence should be addressed; e-mail: sre1@cam.ac.uk.*

Abstract

The development of non-invasive analytical methods is of widespread interest to the field of conservation science, providing chemical insight into the materials used to create painted works of art, which can, for example, inform decisions about their restoration and preservation, or help discern original works from forgeries. A key undertaking in this area is to develop practical methods for identifying and understanding the chemical processes that occur in paint films under ageing. Furthermore, whereas a number of scientific studies have focussed on model systems in which natural ageing processes are simulated in a short time by irradiation under ultraviolet (UV) light, it remains to be established to what extent natural and accelerated ageing induce similar chemical changes. In this work, we employ FT-Raman spectroscopy, together with a simple spectral-deconvolution algorithm, to study in detail the spectral changes accompanying the natural and UV-accelerated ageing of simulated medieval paint films. We find that the two processes differ significantly, and that spectroscopic signatures, principally in the fluorescence background, can thus be used to differentiate the two modes of ageing and hence possibly to identify attempted forgeries. Our studies also suggest that paints based on proteinaceous binders are more stable to ageing than lipid-bound ones. Finally, we investigate the possibility of using our chemometric deconvolution technique, in conjunction with multivariate analysis, for the semi-automated characterisation of the degree or extent of ageing in unknown samples.

Keywords: paint-binder analysis, FT-Raman spectroscopy, UV-accelerated ageing, chemometrics, principal-component analysis, background fluorescence, fibre-optic reflectance spectroscopy

Highlights

- 1) A heuristic spectral-deconvolution algorithm is presented and applied to the analysis of FT-Raman spectra from simulated medieval paints.
- 2) UV-accelerated ageing differs from natural ageing processes, due principally to the apparent formation of C-C triple bonds.
- 3) The fluorescence background of Raman spectra contains information that can help to identify the nature of the ageing (e.g. natural or UV-accelerated).
- 4) Proteinaceous binders are more stable to ageing than are lipidic media.

Introduction

Understanding and identifying the colour palettes and painting techniques used in a piece of artwork can be key to identifying the artist or studio responsible for its creation. Since most works of art have survived the ravages of time, they will invariably show considerable signs of ageing. Understanding the nature of the ageing processes can not only help conservators to develop methods to restore and preserve cultural-heritage objects, but can also help to distinguish newly-forged copies and real old masterpieces.

Ageing encompasses a set of physiochemical processes that paintings undergo within months to years of their making. Initially, the paint, which is a mixture of pigments in a binder or a mixture of binders, undergoes drying. During this process, the solvents from the paint binders evaporate, and the binding medium forms a polymeric matrix[1]. Longer-term ageing leads to various different phenomena, and these have been studied extensively for easel and panel paintings[2-5]. The most commonly-observed process is the oxidative degradation of unsaturated fatty acids in lipidic binders, resulting in the formation of mono- and di-carboxylic acids with varying chain lengths[6, 7]. The species found most commonly, e.g. through GC-MS and FTIR analyses, are azelaic acid (C9), sebacic acid (C10), suberic acid (C8), acetic acid, oxalic acid and glycerol[7, 8]. The smaller acids and glycerol evaporate from the surface of the paintings, while the longer-chain di-carboxylic acids form 3D polymeric networks with the pigments, with the mono-carboxylic acids acting as terminal groups[9]. This phenomenon of cross-linking strengthens the paint layer and prevents its breakdown[9].

However, depending on environmental conditions, the mono-carboxylic acids can form soaps with lead pigments, which migrate to the top layer and frequently form protrusions. This phenomenon is known as the “lead-white phenomenon”[8]. The hydrolysis of polysaturated triglycerides is known to happen over a time-span of 50-100 years and, in the advanced stages of degradation, lead soaps form semi-crystalline structures which eventually flake off[10]. Lead soaps with longer fatty acids behave like liquid crystals and, at higher temperatures, become disordered, leading to solvent uptake and consequent swelling. This form of degradation is frequently noticed in works that have undergone multiple hot-relining operations and exposure to solvents[11].

In 2005, Hoogland and Boon established that lead soaps form only in the presence of hydrolysed acids, as their efforts directly to synthesize lead tripalmitate failed, whereas lead palmitate formed readily from lead carbonate[9]. The formation of lead soaps has been shown to be accelerated at elevated temperatures and high relative humidity[12]. The dynamic process of lead-soap formation has, however, not yet been studied quantitatively, although Cotte *et al.* carried out a kinetic study of lead-soap formation and established that the phenomenon requires only weeks, rather than centuries, to happen, and showed that increased water content accelerates the ageing process[13].

Metal-soap formation was first noticed with lead paints, but many other metal ions also lead to saponification of paint binders. For example, copper, zinc, iron, aluminium, calcium and potassium also form metal carboxylates[14]. Potassium[15, 16] and aluminium[15, 16] ions form soaps which are water soluble and hygroscopic, respectively, and which typically make oil paints unstable to moisture, whereas calcium soaps are more rigid and act to stabilize the paints[17]. In general, degradation processes cause paint films to become thinner and more transparent to light, which is then absorbed by the support layer, making the painting appear darker[8].

Bonaduce *et al.* found that the ageing/hydrolysis pathways of binders were dependent more on the nature of the bound pigment, and less on their pre-processing (e.g. cold pressing, water washing, *etc.*)[18]. It was noted that, of various lead pigments in use, lead white (PbCO_3) reacted most readily to form soaps, forming hydrocerussite nanocrystals, with lead chloride sometimes also being present[19]. Red lead (Pb_3O_4) was found to be the next most efficient at saponification, with the pigment initially converting to lead white, which then subsequently forms lead soaps[20, 21]. Lead-tin yellow (Pb_2SnO_4), however, was found to react more slowly. This pigment leaches out[21], forming a network surrounding the lead soaps, and this remineralisation leads to a coarser-looking paint, sometimes found above the protective layer of varnish. Some artists deliberately made use of this phenomenon to paint lemons[10].

Compared to their lipidic counterparts, ageing of proteinaceous binders is a lot less well understood. Colombini *et al.* carried out extensive analysis on proteinaceous binders using HPLC and GC in conjunction with UV-Visible or IR spectroscopy. They carried out hydrolysis of the samples to free the amino acids before analysis, and used characteristic amino-acid ratios to identify the proteins initially present[22], finding that the composition of the fresh and aged proteinaceous binders did not vary significantly. However, on ageing, these binders form cross-linked polymers with the cations from the pigments, making the recovery of the amino acids more challenging. Moreover, the need to subject the samples to hydrolysis under harsh acidic or basic conditions before they can be analysed using HPLC or GC[22] means that this method is not well suited to analysing cultural-heritage objects.

Ageing of paints can, in general, be affected by humidity, temperature and light conditions, and most studies have been carried out on binders that are oils and other fatty acids, where the yellowing and cracking of paints is apparent[23]. However, while proteinaceous binding media are observed to be relatively stable, not much work has been done to understand their ageing. Manzano *et al.* recently carried out studies on mixtures of lipidic paint binders using Raman spectroscopy and chemometrics[24], during which they identified a need to study the ageing of proteinaceous binders, but observed no systematic chemical changes under accelerated ageing with UV light.

In terms of techniques, a lot of work has been done to investigate ageing processes using FT-IR[5, 25, 26], GC-MS[25, 27, 28], XRF[2, 5], synchrotron radiation (XRD and FTIR)[3] and Raman, both on samples aged naturally for up to five years or longer, and on samples acceleratively aged under UV light[23]. However, little work has yet been done to compare the differences in the nature of ageing under these two regimes. In this work, we present a comprehensive study of the ageing of simulated medieval paint films under both conditions. We make use of FT-Raman spectroscopy, together with a custom-written spectral-decomposition algorithm, to obtain chemometric information on the chemical processes underpinning the ageing. This is backed by complementary fibre-optic reflectance spectroscopy, which provides quantitative information about colour in addition to chemical composition. With these techniques, we perform a detailed comparison of the two ageing methods, and, through analysis of the processes involved, we show that the two leave distinct chemical “signatures”. Finally, building on previous work[29], we also make use of multivariate analysis with different spectral information, to see whether such techniques could be used automatically to differentiate between different ageing processes.

Experimental

Sample Preparation

Paints of three commonly-used lead pigments, *viz.* lead white (LW; PbCO_3 - anhydrous lead carbonate or cerussite), red lead (RL; Pb_3O_4 - lead tetraoxide) and lead-tin yellow (LTY; Pb_2SnO_4 - lead stannate), were prepared using seven different binders, *viz.* egg yolk (EY), egg white (EW), whole egg (WE), gum arabic (GA), linseed oil (LO), poppy oil (PO) and walnut oil (WO), and painted on microscope glass slides. We prepared two sets of each paint sample close to the extremes of the workable-mixture ranges - one set with a high pigment-to-binder ratio (i.e. ‘lean’ in binder), and another with a low pigment-to-binder ratio (‘rich’ in binder).

These were left exposed to sunlight indoors behind a window for one year to allow for natural ageing. After collecting spectra from these samples, they were then subjected to accelerated ageing under a 254 nm ultra-violet light (8W) in a home-made ageing chamber (see supporting information) for one week. The relative humidity and temperature in the chamber were maintained at 34% and 18.8 °C, respectively, with less than 1% variation (see supporting information). The use of 254 nm light is particularly harsh, but was chosen to represent a “worst-case scenario”.

All the pigments used in this study were purchased from Kremer Pigments, Inc., and were used without any further processing. The seven binder materials were purchased locally, except for gum arabic resin (Kordofan Grade), which was imported from the Middle East via L. Cornelissen and Son, London. The GA binder was

prepared from this resin by dissolving it in water. EW, EY and WE binders were made from free-range eggs, while LO, PO and WO were obtained as cold-pressed products.

Spectroscopy

FT-Raman spectra within the spectral range of 20-3600 cm^{-1} were collected using a Bruker Ram II instrument (1064 nm excitation wavelength, ~ 1 mm spot size, KBr beam splitter and Ge detector, 2.37 mm penetration depth) at a resolution of 4 cm^{-1} . The spectra were acquired with an excitation power of 50 mW and integrating 256 scans, as the previously optimised[29] 100 mW laser power was found in preliminary measurements to cause burning of some samples, especially in areas of the films with ‘bubble-like’ protrusions.

Fibre-optic reflectance spectra were obtained using a FieldSpec 4 spectroradiometer (ASD Inc., USA) in the wavelength range 350–2500 nm at a spectral resolution of 3 nm at 700 nm and 10 nm at 1400 nm and 2100 nm. The instrument was calibrated using a 99% reflective spectralon standard (Labsphere) before acquiring sample spectra.

Spectral Decomposition

To aid the analysis of our FT-Raman spectra, we implemented a spectral-decomposition algorithm in the Python 3 programming language[30], using the NumPy[31], SciPy[32] and Matplotlib[33] packages. The code attempts to decompose input spectra into a sum of Lorentzian peak functions and a background polynomial, which can then be analysed separately (e.g. treating the parameters of the Lorentzian functions as a peak table), or combined to yield a smooth approximation of the original spectra.

In the first step, the algorithm attempts to fit the spectral background. Prior to the fitting, it is necessary to exclude data points which are part of prominent peaks, since such features can significantly skew the fit. To do this, the spectrum is divided into N segments (here 5), and the intensities within each fitted to a straight line, $y = mx + c$. Data points lying above a threshold multiple (here 1.05) of this baseline are considered to form part of peaks, and are excluded. The segments are then recombined, median filtered to remove spikes from peak bases, and an n^{th} -order polynomial fitted through the remaining data points. In this work, we used an 11-point median filter, and fitted to a polynomial of degree 10.

In the second step, the algorithm attempts to detect peaks, and to fit them to (scaled) Lorentzian functions. The polynomial obtained in the first step is subtracted from the input spectrum, yielding a background-corrected set of intensities. The corrected spectrum is then analysed over user-defined regions of interest (ROIs), which can optionally be interpolated onto a regularly-spaced grid. The spectra are smoothed using a triangle filter, for which

we found a filter size of 21 data points gave a good balance between reducing noise while preserving features. For peak detection, a baseline slope is obtained from a linear fit, with bands whose intensity is less than a set multiple of the mean (here 1.05) being excluded in a similar manner to the background fitting. Next, the locations of peak centres are identified from maxima which lie at a user-defined multiple (here 1.75) above the baseline.

A sum of Lorentzian functions, one for each peak, is then constructed, with the peak centres and scaling factors estimated based on the raw spectral intensity at the peak position, and the width set by a supplied initial estimate (1 cm^{-1} in the present work). The set of peaks are then optimised against the background-corrected (non-smoothed) spectrum using a least-squares algorithm. To avoid the peak shapes being skewed by high levels of background noise, the spectrum is “zeroed” prior to fitting by subtracting a third linear fit of points lying below a multiple (1.1) of the mean. In some cases, it was found that peaks barely above the baseline produced, on optimisation, spurious broad Lorentzians with centres outside the ROI, and sometimes, as a result of the zeroing, with negative scale factors; therefore, the scale factors were constrained to be positive, and peaks with centres outside the ROI were discarded after the fit.

Each of the stages in the complete algorithm is illustrated for a representative sample spectrum in Figure 1. The output is a peak table, containing the wavenumber, intensity and full width at half maximum (FWHM) of each detected feature, plus the coefficients of the background polynomial. This information can be used to construct various derivative spectra, including a background-corrected version of the original, and smooth pure “background” and “peak” spectra, plus a smooth “chemometric spectrum” consisting of the peaks plus the background function.

This algorithm is purely “heuristic” (i.e. implements a human-like approach), and requires several input parameters to be tuned for optimal results, some of which could potentially be determined automatically or assigned values based on other input parameters. However, we found that this algorithm fared significantly better than arguably more elegant algorithms (e.g. [34]) when used with noisy spectra, such as are typically obtained from complex mixtures like those analysed in the present study. The parameters listed in the above description were found to work well across the broad range of samples we studied, generally successfully identifying and fitting the major peaks and background while omitting spurious features close to the level of the background noise.

Principal-Component Analysis

Multivariate analysis of spectral data was performed using the Matplotlib[33] principal-component analysis (PCA) functionality, with pre-processing and data-handling routines implemented in Python 3. FT-

Raman spectra were first smoothed with a 21-point triangle filter and vector normalised, as described in our previous study[29]. This filter and window width were selected to achieve a good balance between preserving spectral features and removing noise. FT-Raman spectra, including the various processed spectra generated by the spectral-decomposition routine, were analysed with fibre-optic reflectance data, again as described in Ref. [29]. The region of the FT-Raman spectra between 1100 and 3200 cm^{-1} , i.e. above the fingerprint region, was taken for the Raman analyses, leaving out the prominent peaks from the pigments that arise in the low-wavenumber regions, while the complete FORS spectra were used in the analyses.

Before the construction of PCA-training matrices, spectra were interpolated to a common set of bands; in the composite Raman/FORS spectra, 500 data points from Raman and 1000 data points from FORS were used in each data set. The choice of the numbers of data points was made based on the resolution of the input spectra and on keeping the computational and memory requirements of the PCA manageable. While we found that using a low number of data points (< 500 in total) adversely affected the quality of the PCA, at the interpolation resolution adopted in this study adding additional data points had no visible effect[29].

Results and Discussion

FT-Raman Spectra

Representative FT-Raman spectra of the 42 paints analysed in the present study (three pigments with seven binders in two concentrations), as prepared and following natural and UV-accelerated ageing, are shown in Figs. S3-S8, and corresponding spectra recorded from paint-outs of the pure binders are compared in Fig. S9. The quality of the spectra was found to depend on the pigment/binder combination, with some samples yielding relatively smooth spectra with sharp features, while the spectra of others displayed high levels of background noise. In many cases, we found that ageing led to a reduction in band intensity, often accompanied by the broadening of weaker spectral features which, in some cases, led to their being barely visible above the background noise. It was observed that some of the binder-rich paint samples peeled away from the substrate, and some were notably darkened (see supporting information) on visual examination.

The peak-detection method and background-correction algorithms were used to identify prominent peaks, which were verified by eye and then assigned to the corresponding functional groups[24, 35, 36]. Assignments were restricted to the region between 1100 and 3200 cm^{-1} , as this is above the region where the phonon bands from the pigments occur, and only peaks relating to changes induced by ageing are discussed here.

The most interesting feature found to arise from ageing was the appearance of peaks between 1900 and 2100 cm^{-1} , which are indicative of C=C and partial triple bonds. These were clearly noticeable in the spectra of

UV-aged samples of pure binders (both lipidic and proteinaceous), as exemplified in Figure 2, and also in spectra of LW and LTY paints, but were less prominent in spectra of RL paints. They were not observed in the spectra of naturally-aged paints, which suggests that the chemical changes induced by these two modes of ageing are significantly different. On UV-accelerated ageing, it is probable that the top layer of paint undergoes oxidative degradation, resulting in the formation of species containing double and triple C-C bonds. This is consistent with reports of differential changes in the compositions of the top and bulk layers of paint on accelerated ageing, with the absence of short-chain acids on the top layer identified using secondary ion mass spectrometry (SIMS)[37].

Another prominent spectral feature is the appearance of CH₃ rocking vibrations in both sets of aged paints, which were not observed in the fresh paints analysed in our previous study[29]. Carbonyl peaks were also found generally to have broadened so much as to be lost in the background noise, and were observed as clear peaks in only a small subset of the spectra, e.g. in the PO- and LO-based paints. This has been reported in similar studies using FTIR spectroscopy[38]. Similarly, the amide I and III bands between ~1280 and 1650 cm⁻¹ were absent in the aged samples, possibly due to broadening, and were observed only in one or two spectra of EW- and EY-based paints.

As observed in other studies[8], carboxylate peaks due to C-O-C bond vibrations were visible at ~1100 cm⁻¹ in the LW- and LTY-based paints made with lipidic binders. These features were not observed in the spectra of paints based on aged proteinaceous binders, which have been observed to be much more stable to ageing than lipidic binders, which typically degrade and form metal soaps. In a few of our LW and RL paints, the Raman excitation laser caused visible degradation at some spots, resulting in the formation of PbO, indicated by the appearance of characteristic phonon bands at 84 and 138 cm⁻¹[39]. These also clustered separately in the PCA score plots (see below), giving rise to multiple clusters for these paint samples, which suggests that the laser also caused damage to the binding media and consequent changes to the higher-frequency regions of the spectrum.

Background Fluorescence

It is a common practice when processing Raman spectra to remove the background (generally assumed to be principally due to fluorescence) in order to improve the clarity of the spectral features. However, it is quite conceivable that the combination of processes contributing to the background fluorescence could itself act as a signature of the material under study.

To investigate this, we compared the background polynomials extracted from the chemometric decomposition of the spectra of our binder-rich LW paints (Figure 3). In the naturally-aged paints, the background fluorescence is consistently centred around 1500 cm^{-1} . Accelerated ageing appears to lead to a general increase in the height of the fluorescence background, particularly noticeable for the EW and WO spectra, and in some cases also causes a shift to higher wavenumbers. It is noteworthy that the equivalent fresh samples analysed in our previous study[29] generally did not display such prominent fluorescence backgrounds, and thus this appears to arise to some extent as a result of ageing. The differences in features observed here between naturally- and artificially-aged paints are quite similar to the observations of Osticioli *et al.*[42] from fluorescence-spectroscopy studies, although these were performed with a 230 nm excitation-laser wavelength, and the fluorescence was observed at 380 nm ($26,316\text{ cm}^{-1}$, a response attributed to the amino acid tryptophan), i.e. far from the spectral region being analysed in the present work.

The changes to the background fluorescence, particularly on accelerated ageing, appear to be a consistent trend for the LW paints, bar the LW-WO combination, the reasons for which are not currently well understood. The trends can be more clearly seen from a quantitative comparison of the positions of the maxima in, and areas under, the fluorescence backgrounds (see supporting information), which further shows that the increase in the fluorescence background on UV-accelerated ageing is more prominent in paints rich in binder than in paints lean in binder. In the case of the latter, the lipidic binders produce more fluorescence than do the proteinaceous ones. This suggests that the LW paints with lipidic binders undergo ageing faster than do proteinaceous ones. Similar phenomena were also noticed in the RL- and LTY-based paints (see supporting information), although the effect was not as prominent as with LW.

These findings, together with those in the previous section, suggest that an analysis of the spectral background could potentially be used in conjunction with other spectral features to determine the conditions under which a painting has been aged. The form of the background could thus contain vital clues for discerning century-old masterpieces from newly-forged counterparts, even in challenging cases where the forgers succeed in replicating the artists' colour palette.

Fibre-Optic Reflectance Spectra

Representative FORS spectra of the fresh and aged paints and pure binders analysed in this work may be found in Figs. S10-S16. As in the case of the Raman spectra, we discuss only those changes attributed to ageing; an analysis of the spectra of the fresh samples may be found in Refs. [40, 41]. The FORS spectra from several of the systems analysed in the present work display interesting contrasts between the as-prepared, naturally-aged and UV-aged samples. The lipid-based binders were found to have lost peaks related to the overtone vibrations of $-\text{CH}_3$, $-\text{CH}_2-$ and $-\text{CH}=\text{CH}-$ groups, which occur between 1725 to 1760 nm, and also those from $-\text{CH}_2-$ and $-\text{CH}_3$

combination bands at ~ 2350 nm. The band at 2305 nm, which is characteristic of the presence of lipidic species, was present in the spectra of these samples, but in most cases was very weak. In contrast, spectra from paints made up with proteinaceous binders and aged using the two different methods did not show any notable differences in spectral features compared to one another.

Multivariate Analysis

In our previous work[29], we highlighted the utility of multivariate analysis for differentiating between different binding media used to prepare paint samples. The main objectives of this section are to investigate to what extent this is still possible in the presence of ageing, whether multivariate techniques can discriminate between the binders, modes of ageing, and also whether the signal processing facilitated by the chemometric-decomposition routine can improve sample classification. As in our previous study[29], we found that combined FT-Raman and FORS spectra generally facilitated better classification when used with PCA, and thus these spectra were used for all our analyses.

We first investigated whether PCA could differentiate different binders in different concentrations for each pigment in the presence of natural and UV-accelerated ageing. Figure 4 compares analyses of the naturally and UV-aged RL paints, with the FT-Raman data background corrected or converted to smooth chemometric representations from the fitted background and peak functions. In the analyses of the naturally-aged samples, we found that the different binders/concentrations formed fairly-well separated bands when background-corrected Raman spectra were used, whereas using the chemometric spectra led to tighter and often overlapping clusters. For the UV-aged samples, the background-corrected spectra likewise led to the most distinct clustering, although unlike with the naturally-aged samples, these were generally less well separated.

The loading plots for these PCAs (Figure 5) generally show equal weights for FORS and Raman spectra in the first two principal components (PCs). When the background-corrected FT-Raman data are used to analyse the UV-aged paints (Fig. 4b), features between 2000 and 2500 cm^{-1} in the Raman spectra, indicative of C-C double and partial-triple bonds are weighted in both PCs, most notably PC2, whereas this is not apparent in the analysis of the naturally-aged paints. This contrasts with a similar analysis of the naturally-aged LW paints (see supporting information), where these features appear to be evident and can be used for discrimination, which confirms that LW leads to faster ageing, as previously reported in the literature[8]. It has also been reported that paints which have a lower lead content (i.e. as is the case with the binder-rich samples in the present work) undergo faster ageing[9]. The loading plots for the analyses performed with the chemometric spectra, on the other hand, do not appear to display any prominent features in the C-C multiple-bond region, which suggests that the

relatively poorer grouping of samples in the PCA plots may be due to the chemometric decomposition failing to identify subtle peaks close to the background noise for samples where ageing leads to such poor-quality spectra.

When analysing cultural-heritage objects, a likely scenario is that the pigment and class of binder (e.g. proteinaceous or lipidic) would be known, e.g. from provenance, visual inspection or other analytical techniques, but the exact binding material and degree of ageing would not. We therefore performed separate PCAs on paints made up with lipidic and proteinaceous binders separately (Figures 6a and 6b). Figure 6a analyses lipidic LW paints, and shows that the multivariate analysis is able fairly well to separate out the different binders, modes of ageing and paint/binder compositions. There is a visible tendency for the UV-aged samples to cluster close together, suggesting that the processes induced by ageing (e.g. the formation of metal soaps) are similar for all three oils, and are prominent in the spectra. The loading plots (see supporting information) show that PC1 gives more weight to the FORS spectra, and PC2 more weight to the Raman spectra. In the Raman spectra, we found that, aside from in the C-H stretch region, the bases of the peaks were invariably weighted more highly than the peaks themselves, which is consistent with spectral broadening being a primary feature induced by ageing.

On the other hand, the analysis carried out on RL paints in proteinaceous binders (Figure 6b) shows well-defined clusters for both the naturally aged and the UV-aged samples. Even though the WE, EW and GA paints fall close to one another, they form distinguishable clusters. In keeping with the attribution of the similarity of UV-aged lipidic LW paints to the chemical changes induced by the ageing processes, it has been previously shown that proteinaceous binders are more stable to ageing than the lipidic ones[23], which could explain the improved sample grouping in this analysis.

Finally, to further test the possibility of using the spectral-decomposition method for improving classification in multivariate analyses, a PCA was performed on spectra of UV-aged LW paints composed solely of smooth peak functions (Figure 6c). We chose this set of paint samples as they have been shown to undergo the most facile ageing[8], and thus should best display the chemical changes involved. As observed in Figure 6a, the similar ageing of the lipidic binders led to close clustering, although, on expanding this region of the plot, they were observed to form distinguishable clusters. Unlike the lipidic binders, the EW and WE points displayed a large spread. The loading plots (see supporting information) show that, in this analysis, PC1 gives more weight to the SWIR region of the FORS, with PC2 weighting the Raman spectra. The weights in the Raman spectra tend to extend over the peak bases, again highlighting peak broadening as a key fingerprint in FT-Raman data, and, interestingly, a lower weight is assigned to the C-H region in comparison to the other regions. The improved ability of this analysis to differentiate between aged lipidic binders suggests that the information from the chemometric decomposition could be useful for analysis in certain cases.

Conclusions

In summary, we have carried out a comprehensive spectroscopic study of the effects of natural and UV-accelerated ageing on lead-based paints, made up with three widely-used Medieval pigments and seven binders, using FT-Raman and fibre-optic reflectance spectroscopy. We have also developed a heuristic spectral-decomposition algorithm, which is robust to moderate levels of background noise, and which was successfully used to assist with the interpretation of the Raman spectra.

Our observations of the chemical effects of ageing are generally in line with the findings of other studies, for example that the presence of lead white accelerates ageing, and that proteinaceous binders are more stable to ageing than lipidic ones. We also found that the fluorescence background in FT-Raman spectra could potentially act as a signature of the extent and type of ageing that a paint has undergone, and hence that this often-discarded part of the spectrum may provide valuable information for the analysis and preservation of cultural-heritage objects.

Finally, we also demonstrated that the multivariate analysis techniques developed in previous work, based on principal-component analysis of combined FT-Raman and FORS spectra, can be applied to aged as well as fresh samples. This highlights the robustness of this approach for the classification of paint samples using non-invasive and portable spectroscopic techniques. The chemometric-decomposition algorithm, used to pre-process the FT-Raman data (e.g. by removing the fluorescence background), can also in some cases be used to improve the discrimination between sets of samples in these analyses.

Overall, this work highlights the utility of spectroscopy in conservation science, and illustrates how combining data from complementary techniques with suitable analysis tools might in the future be used for the automated characterisation of e.g. works of art against a database of references.

Data-Access Statement

A subset of the data analysed in this manuscript is available online, free of charge, from [URL to be added on acceptance]. This includes representative FT-Raman and FORS spectra from the various paint samples studied in this work, plus data from the PCAs discussed in the text and supporting information. Other data are available from the authors on request.

Notes and References

Electronic supporting information is available online at [URL inserted by publisher] or from the authors.

- [1] Boon J J, Peulve S, Van den Brink O F, Duursma M C and Rainford D 1997 Molecular aspects of mobile and stationary phases in ageing tempura and oil paint films, in early Italian paintings: Techniques and analysis. (Maastricht: Limburg Conservation Institute (SRAL)) pp 35-56
- [2] Faubel W, Simon R, Heissler S, Friedrich F, Weidler P G, Becker H and Schmidt W 2011 Protrusions in a painting by Max Beckmann examined with confocal mu-XRF *Journal of Analytical Atomic Spectrometry* **26** 942-8
- [3] Salvado N, Buti S, Nicholson J, Emerich H, Labrador A and Pradell T 2009 Identification of reaction compounds in micrometric layers from gothic paintings using combined SR-XRD and SR-FTIR *Talanta* **79** 419-28
- [4] Cotte M, Susini J, Sole V A, Taniguchi Y, Chillida J, Checroun E and Walter P 2008 Applications of synchrotron-based micro-imaging techniques to the chemical analysis of ancient paintings *Journal of Analytical Atomic Spectrometry* **23** 6 820-828
- [5] Cotte M, Checroun E, Susini J and Walter P 2007 Micro-analytical study of interactions between oil and lead compounds in paintings *Applied Physics a-Materials Science & Processing* **89** 841-8
- [6] Verhoeven M A, Carlyle J, Reedijk J and Haasnoot J G 2006 Exploring the application of solid state nuclear magnetic resonance to the study of the deterioration of paintings MOLART report 13. In: *Reporting the Highlights of the De Mayerne Program*, pp 33 - 43
- [7] Plater M J, De Silva B, Gelbrich T, Hursthouse M B, Higgitt C L and Saunders D R 2003 The characterisation of lead fatty acid soaps in 'protrusions' in aged traditional oil paint *Polyhedron* **22** 3171-9
- [8] Mazzeo R, Prati S, Quaranta M, Joseph E, Kendix E and Galeotti M 2008 Attenuated total reflection micro FTIR characterisation of pigment-binder interaction in reconstructed paint films *Analytical and Bioanalytical Chemistry* **392** 65-76

- [9] Boon J J, Hoogland F and Keune K 2006 Chemical processes in aged oil paints affecting metal soap migration and aggregation. In: *34th annual meeting of the AIC of Historic & Artistic Works providence*, ed H M Parkin (Rhode Island pp 16-23)
- [10] Noble P, Boon J J and Wadum J 2002 Dissolution, Aggregation and protrusion: Lead soap formation in 17th century grounds and paint layers *Artmatters 1* 46 - 62
- [11] Middlekoop N, Noble P, Wadum J and Broos B Rembrandt under the scalpel: The anatomy of lesson of DR. Nicolaes Tulp dissected. (Amsterdam / The Hague pp 56, 7, 66)
- [12] Carlyle L 2006 Historically accurate reconstructions of oil painter's materials: an overview of the Hart project 2002 -2005. In: *Reporting Highlights of the De Mayerne Program - MOLART Report 13*, pp 63 - 77
- [13] Cotte M, Checroun E, Susini J, Dumas P, Tchoreloff P, Besnard M and Walter P 2006 Kinetics of oil saponification by lead salts in ancient preparations of pharmaceutical lead plasters and painting lead mediums *Talanta* **70** 1136-42
- [14] Spring M H, C.Saunders, D. Investigation of paint-medium interaction processes in oil paint containing degraded smalt. 2005 *National Gallery Technical Bulletin* **26** 56-69
- [15] Boon J J, Keune K, van der Weerd J, Geldof M and de Boer J 2001 Imaging microspectroscopic, secondary ion mass spectrometric and electron microscopic studies on discoloured and partially discoloured smalt in cross-sections of 16th century paintings *Chimia* **55** 952-60
- [16] Sister D and Minopoulou E 2009 A study of smalt and red lead discolouration in Antiphonitis wall paintings in Cyprus *Applied Physics a-Materials Science & Processing* **96** 701-11
- [17] Burnstock A, Van der Berg K J, De Groot S and Wijnberg L 2006 An investigation of water sensitive oil paints in 20th century paintings. In: *Modern Paints Uncovered conference*, ed T In Learner (London: Getty Publication) pp 177-88.
- [18] Bonaduce I, Carlyle L, Colombini M P, Duce C, Ferrari C, Ribechini E, Sella P and Tine M R 2012 A multi-analytical approach to studying binding media in oil paintings: Characterisation of differently pre-treated linseed oil by DE-MS, TG and GC/MS *Journal of Thermal Analysis and Calorimetry* **107** 1055-66
- [19] Pina C M, FernandezDiaz L and Prieto M 1996 Topotaxy relationships in the transformation phosgenite-cerussite *Journal of Crystal Growth* **158** 340-5
- [20] Boon J J, Van der Weerd J, Jeune K, Noble P and Wadum J 2003 Mechanical and physical changes in old Master paintings: dissolution, metal soap formation and remineralization processes in lead pigmented ground/ immediate paint layers of 17th century painting. In: *13th Triennial Meeting of the ICOM committee for conservation in Rio de Janeiro*, ed R.Vontobel (London: James & James) pp 401 - 6
- [21] Higgitt C, Spring M and Saunders D eds 2003 *Pigment-medium interactions in oil paint films containing red lead or lead-tin yellow* vol 24 (Italy: Kate Bell)

- [22] Colombini M P and Modugno F 2004 Characterisation of proteinaceous binders in artistic paintings by chromatographic techniques *Journal of Separation Science* **27** 147-60
- [23] Manzano E, Navas N, Checa-Moreno R, Rodriguez-Simon L and Capitan-Vallvey L F 2009 Preliminary study of UV ageing process of proteinaceous paint binder by FT-IR and principal component analysis *Talanta* **77** 1724-31
- [24] Manzano E, Garcia-Atero J, Dominguez-Vidal A, Ayora-Canada M J, Capitan-Vallvey L F and Navas N 2012 Discrimination of aged mixtures of lipidic paint binders by Raman spectroscopy and chemometrics *Journal of Raman Spectroscopy* **43** 781-6
- [25] Katsibiri O and Howe R F 2010 Characterisation of the transparent surface coatings on post-Byzantine icons using microscopic, mass spectrometric and spectroscopic techniques *Microchemical Journal* **94** 14-23
- [26] Kaszowska Z, Malek K, Panczyk M and Mikolajska A 2013 A joint application of ATR-FTIR and SEM imaging with high spatial resolution: Identification and distribution of painting materials and their degradation products in paint cross sections *Vibrational Spectroscopy* **65** 1-11
- [27] Keune K, Hoogland F, Boon J J, Peggie D and Higgitt C 2009 Evaluation of the "added value" of SIMS: A mass spectrometric and spectroscopic study of an unusual Naples yellow oil paint reconstruction *International Journal of Mass Spectrometry* **284** 22-34
- [28] Manzano E, Rodriguez-Simon L R, Navas N, Checa-Moreno R, Romero-Gamez M and Capitan-Vallvey L F 2011 Study of the GC-MS determination of the palmitic-stearic acid ratio for the characterisation of drying oil in painting: La Encarnacion by Alonso Cano as a case study *Talanta* **84** 4 1148-1154
- [29] Pallipurath A, Skelton J, Ricciardi P, Bucklow S and Elliott S 2013 Multivariate analysis of combined Raman and fibre-optic reflectance spectra for the identification of binder materials in simulated medieval paints *Journal of Raman spectroscopy* **44** 866 - 74
- [30] Python Software Foundation, <http://www.python.org>.
- [31] NumPy, <http://www.numpy.org>.
- [32] Scientific Tools for Python, Travis Oliphant, Pearu Peterson *et al.*, <http://www.scipy.org>.
- [33] Matplotlib, <http://matplotlib.org/>.
- [34] Rowlands C J and Elliott S R 2011 Denoising of spectra with no user input: a spline-smoothing algorithm *Journal of Raman Spectroscopy* **42** 370-6
- [35] Nevin A, Osticioli I, Anglos D, Burnstock A, Cather S and Castellucci E 2007 Raman spectra of proteinaceous materials used in paintings: A Multivariate analytical approach for classification and identification *Analytical Chemistry* **79** 6143-51

- [36] Sadeghijorabchi H, Wilson R H, Belton P S, Edwardswebb J D and Coxon D T 1991 Quantitative-analysis of oils and fats by fourier-transform raman-spectroscopy *Spectrochimica Acta Part a-Molecular and Biomolecular Spectroscopy* **47** 1449-58
- [37] Keune K 2005 Binding medium, pigments and metal soaps characterised and localised in paint cross-sections. In: *PhD Thesis - Report - MOLART11, AMOLF, Amsterdamn: University of Amsterdamn*) p 181
- [38] van der Weerd J, van Loon A and Boon J J 2005 FTIR studies of the effects of pigments on the aging of oil *Studies in Conservation* **50** 3-22
- [39] Burgio L, Clark R J H and Firth S 2001 Raman spectroscopy as a means for the identification of plattnerite (PbO₂), of lead pigments and of their degradation products *Analyst* **126** 222-7
- [40] Bacci M, Fabbri M, Picollo M and Porcinai S 2001 Non-invasive fibre optic Fourier transform-infrared reflectance spectroscopy on painted layers - Identification of materials by means of principal component analysis and Mahalanobis distance *Analytica Chimica Acta* **446** 15-21
- [41] Vagnini M, Miliani C, Cartechini L, Rocchi P, Brunetti B G and Sgamellotti A 2009 FT-NIR spectroscopy for non-invasive identification of natural polymers and resins in easel paintings *Analytical and Bioanalytical Chemistry* **395** 2107-18
- [42] Osticioli I, Nevin A, Anglos D, Burnstock A, Cather S, Becucci M, Fotakis C and Castellucci E 2008 Micro-Raman and fluorescence spectroscopy for the assessment of the effects of the exposure to light on films of egg white and egg yolk *Journal of Raman Spectroscopy* **39** 307-13

Figure 1: Illustration of the different steps involved in the spectral-decomposition algorithm, applied to a representative FT-Raman spectrum (lead white in linseed oil). (a) Detection and removal of the spectral background. A ten-power polynomial was used as the background function. (b) Peak detection, with maxima above a set threshold value (indicated by the blue line) in a smoothed approximation of the background-corrected spectrum in (a) being identified as peaks. (c) Components of the deconvoluted spectrum, viz. the background polynomial detected in (a) plus a sum of scaled Lorentzian peak functions. (d) The deconvoluted spectrum, i.e. the sum of the components in (c), compared against the original.

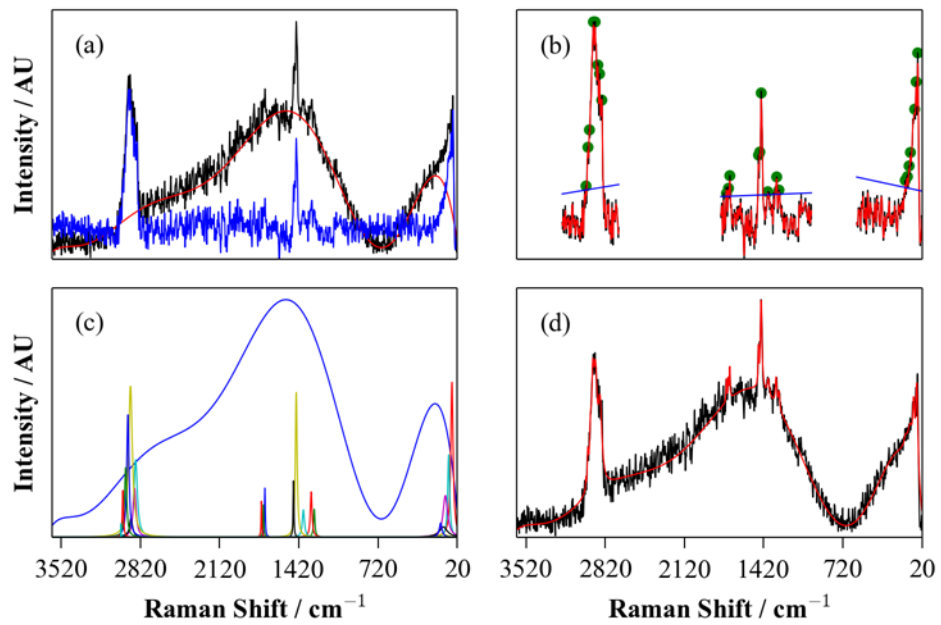
*Figure 2: Representative FT-Raman spectra of UV-aged pure whole egg (a) and walnut oil (b). The peaks marked * indicate those which were identified during the spectral decomposition. As noted in the Experimental section, both spectra were acquired at 50 mW laser power and 4 cm⁻¹ resolution from the integration of 256 scans.*

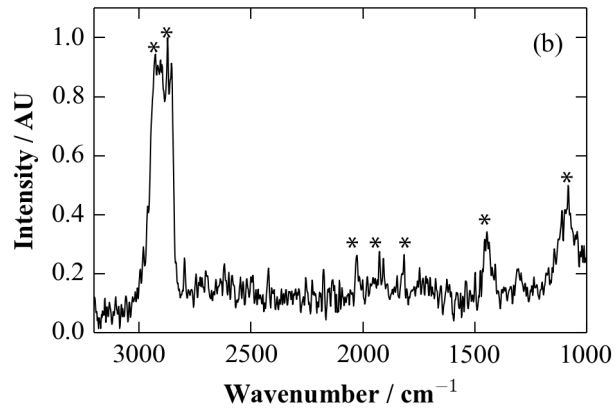
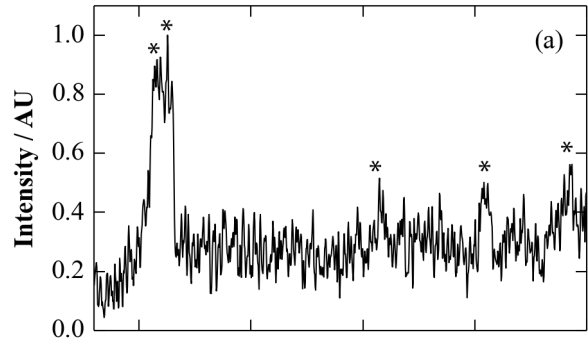
Figure 3: Representative background functions obtained from the chemometric decomposition of FT-Raman spectra of binder-rich LW-based paints after (a) natural and (b) UV-accelerated ageing.

Figure 4: PCAs of combined FT-Raman and FORS spectra of RL paints in all seven binders aged naturally (a, c) and under UV light (b, d). The analyses in (a) and (c) were performed with FT-Raman spectra with the background fluorescence removed, while those in (b) and (d) were performed with the smooth “chemometric” spectra obtained from the spectral-decomposition algorithm. In each plot, filled markers represent samples rich in binder, and hollow markers the corresponding samples lean in binder.

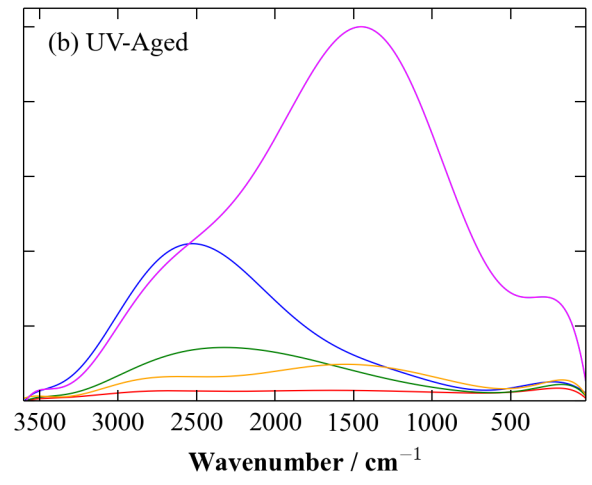
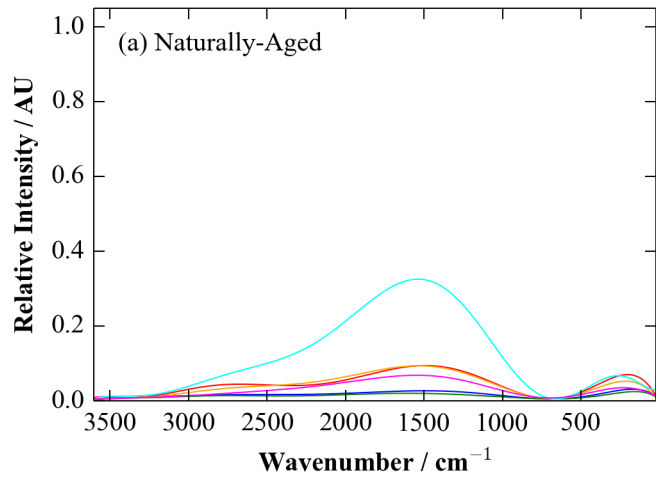
Figure 5: Loading plots showing the weights assigned to the FT-Raman and FORS bands in the first two principal components in the PCAs shown in Fig. 4 (a) - (d).

Figure 6: PCAs of combined FT-Raman and reflectance spectra from (a) naturally-aged and UV-aged LW paints made up with lipidic binders, (b) naturally-aged and UV-aged RL paints made up with proteinaceous binders, and (c) UV-aged LW paints with the seven binders investigated in this study. For analyses (a) and (b), the background-corrected FT-Raman spectra were used, while for (c) a spectrum composed only of the peaks obtained from the chemometric decomposition was used. The markers are coloured according to a two-tone shading scheme. The left-hand portion of the markers corresponding to binder-rich samples are filled, whereas those indicating binder-lean samples are hollow. The right-hand portion is coloured olive green or dark blue to indicate natural or UV ageing, respectively.

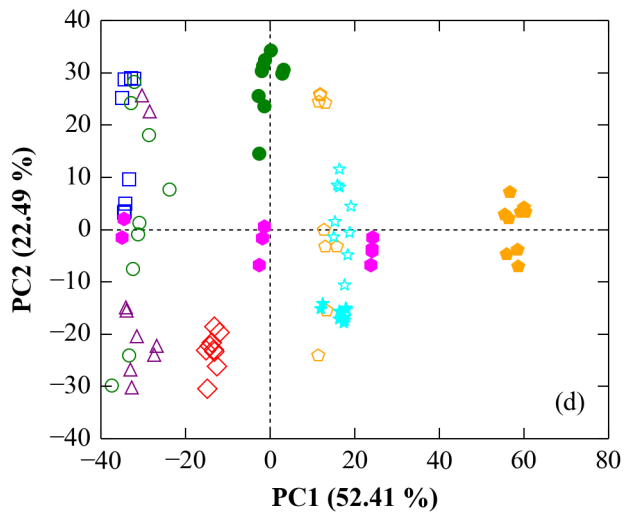
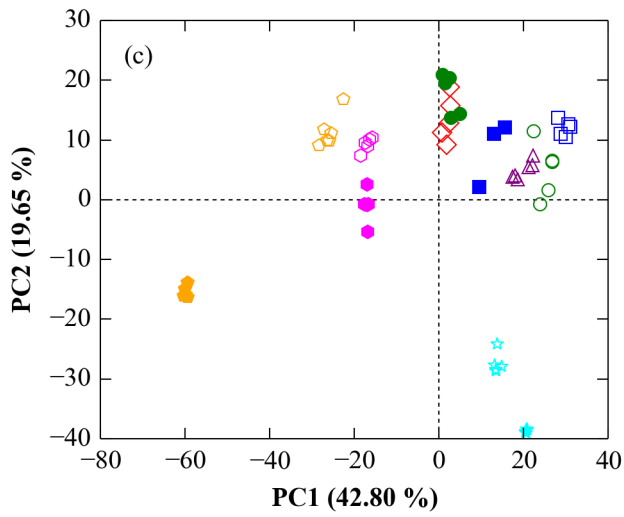
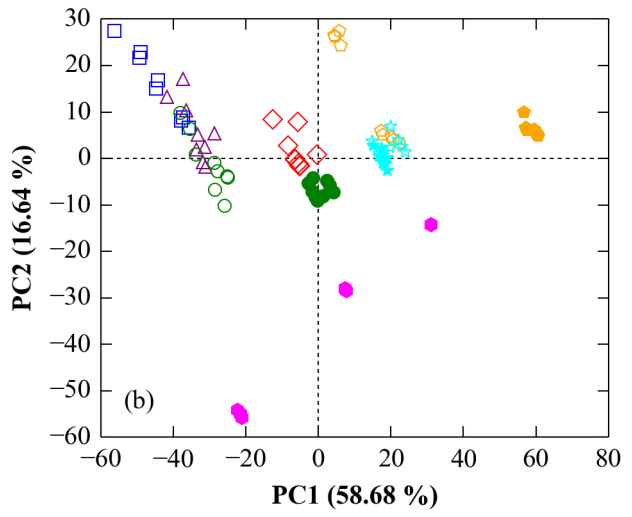
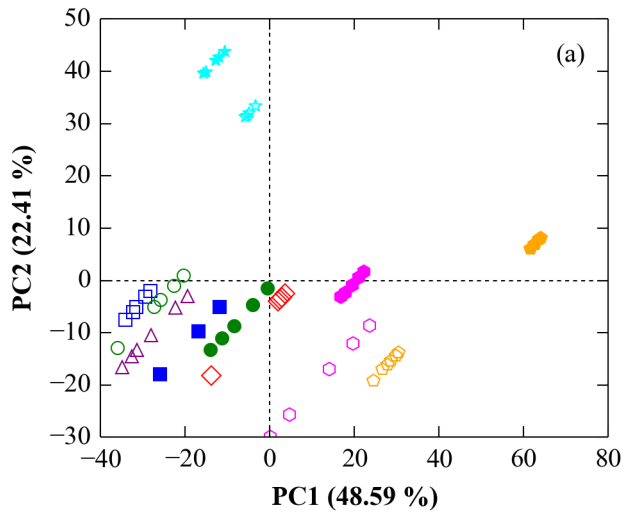


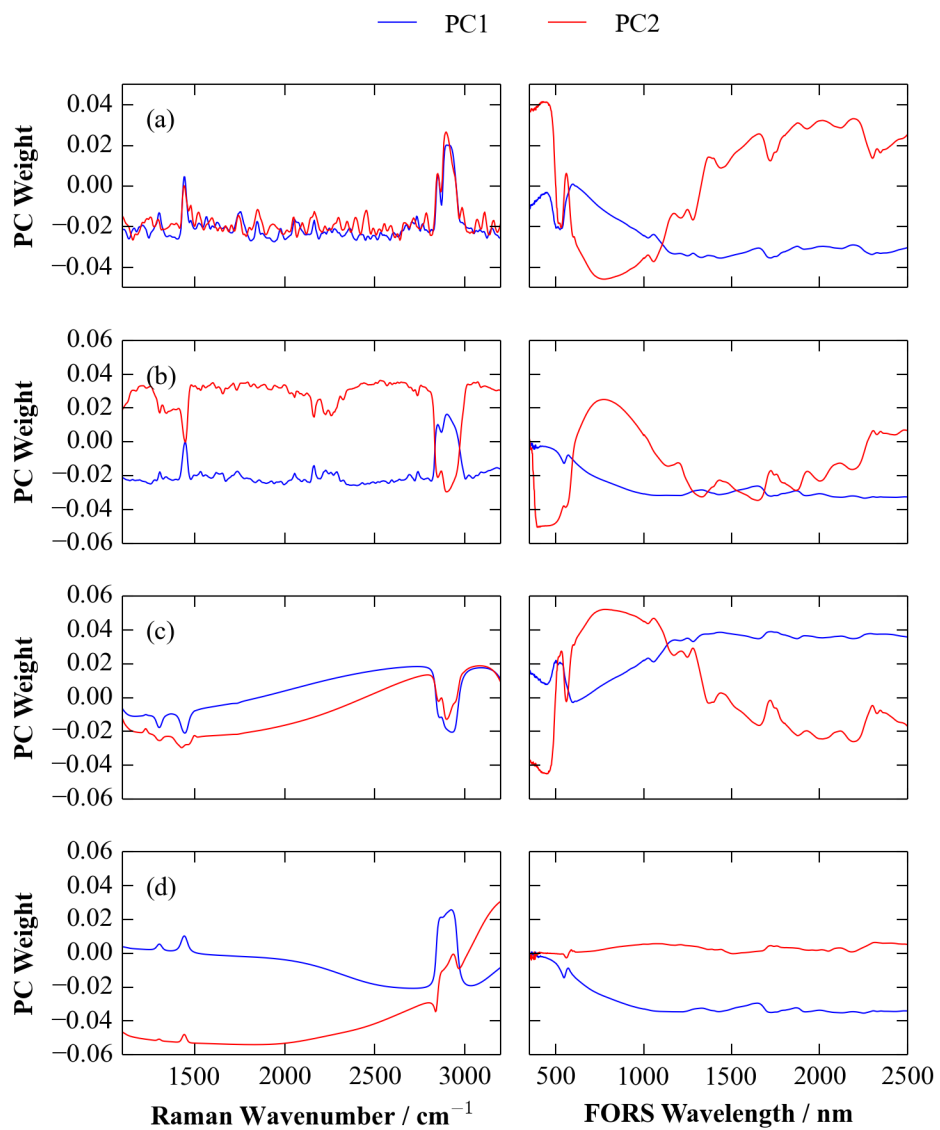


EW EY WE LO PO WO



□ EW ◇ EY ○ WE △ GA ◊ LO ☆ PO ○ WO





◆ na-LO ◆ na-WO ★ uv-PO
★ na-PO ◆ uv-LO ◆ uv-WO

■ na-EW ▲ na-GA ● uv-WE
◆ na-EY ■ uv-EW ▲ uv-GA
● na-WE ◆ uv-EY

